Intramolecular Electron Transfer in Single-Site-Mutated Azurins†

Ole Farver,*,‡ Lars K. Skov,§ Torbjörn Pascher,∥ B. Göran Karlsson,∥ Margareta Nordling,∥ Lennart G. Lundberg,∥ Tore Vänngård,∥ and Israel Pecht⊥

Institute of General Chemistry, The Royal Danish School of Pharmacy, DK-2100 Copenhagen, Denmark, Department of Chemistry, The H. C. Ørsted Institute, University of Copenhagen, DK-2100 Copenhagen, Denmark, Department of Biochemistry and Biophysics, University of Göteborg and Chalmers University of Technology, S-412 96 Göteborg, Sweden, and Department of Chemical Immunology, The Weizmann Institute of Science, Rehovot 76100, Israel

Received September 17, 1992; Revised Manuscript Received March 29, 1993

ABSTRACT: Single-site mutants of the blue, single-copper protein, azurin, from *Pseudomonas aeruginosa* were reduced by CO_2^- radicals in pulse radiolysis experiments. The single disulfide group was reduced directly by CO_2^- with rates similar to those of the native protein [Farver, O., & Pecht, I. (1989) *Proc. Natl. Acad. Sci. U.S.A. 86*, 6968–6972]. The $RSSR^-$ radical produced in the above reaction was reoxidized in a slower intramolecular electron-transfer process (30–70 s^{-1} at 298 K) concomitant with a further reduction of the Cu(II) ion. The temperature dependence of the latter rates was determined and used to derive information on the possible effects of the mutations. The substitution of residue Phe114, situated on the opposite side of Cu relative to the disulfide, by Ala resulted in a rate increase by a factor of almost 2. By assuming that this effect is only due to an increase in driving force, $\lambda = 135$ kJ mol^{-1} for the reorganization energy was derived. When Trp48, situated midway between the donor and the acceptor, was replaced by Leu or Met, only a small change in the rate of intramolecular electron transfer was observed, indicating that the aromatic residue in this position is apparently only marginally involved in electron transfer in wild-type azurin. Pathway calculations also suggest that a longer, through-backbone path is more efficient than the shorter one involving Trp48. The former pathway yields an exponential decay factor, β, of 6.6 nm^{-1}. Another mutation, raising the electron-transfer driving force, was produced by changing the Cu ligand Met121 to Leu, which increases the reduction potential by 100 mV. However, the increase in rate was less than expected from the larger driving force and is probably compensated by a small increase in λ. Marcus theory analysis shows that the observed rates are in accordance with a through-bond electron-transfer mechanism.

Electron transfer proceeding over long distances in proteins plays an important role in biological energy conversion systems such as respiration and photosynthesis. Investigation of the parameters which control long-range electron transfer (LRET)[1] in proteins therefore constitutes an important and interesting subject (Clarke et al., 1991). Azurins are blue, single-copper proteins that mediate electrons in the energy conversion systems of several bacteria (Farver & Pecht, 1984; Adman, 1985). All azurins sequenced to date contain a single disulfide bridge, which is found at one end of the β-sandwich-folded protein at a distance of about 2.7 nm from the copper binding site (Adman, 1985; Baker, 1988; Nar et al., 1991a,b). We have previously shown that this disulfide can be reduced by CO_2^- radicals, produced by pulse radiolysis, to yield a transient $RSSR^-$ radical ion (Farver & Pecht, 1989). This transient decays by an intramolecular electron-transfer process to the Cu(II) center.

We have investigated this intramolecular LRET in distinct azurins isolated from several different bacteria. Azurin thus provides a model system for intraprotein electron-transfer processes of biological interest. The factors that determine the rates of electron transfer within proteins have been shown (Marcus & Sutin, 1985) to be the following: (a) the driving force of the reaction, i.e., the free energy change, $-\Delta G°$; (b) the reorganization energy, λ, associated with changes in intramolecular bond distances and angles as well as changes in the polarization of the medium surrounding the reaction partners; (c) the distance between the electron donor and acceptor; and finally (d) the nature of the microenvironment that separates them. In order to understand the roles of these factors in detail, we have studied the intramolecular LRET process described above in several azurins where single-site mutations have been introduced into the *Pseudomonas aeruginosa* protein. Two of the azurins have single amino acids mutated proximal to the copper site: one where Phe114 was exchanged by Ala (F114A), and the other where Met121 (one of the copper ligands) was substituted by Leu (M121L). These substitutions have been shown to cause changes in the spectroscopic and redox properties of the copper site (Karlsson et al., 1989a, 1991; Pascher et al., 1989). In two other mutated azurins, Trp48, situated midway between the electron donor, $RSSR^-$, and the acceptor, Cu(II), was substituted by non-aromatic residues, Leu (W48L) and Met (W48M), changing the nature of the intervening region between the electron-transfer partners. The rates and amplitudes of the intramolecular LRET in these proteins were studied as a function of concentration, temperature, and pH. The experimental results

† L.K.S. is the recipient of a grant from the Danish Natural Science Research Council. The work was further supported by grants from the German–Israeli Foundation for Scientific Research and Development (I-129) and the Swedish Natural Science Research Council.

‡ The Royal Danish School of Pharmacy.

§ University of Copenhagen.

∥ University of Göteborg and Chalmers University of Technology.

⊥ The Weizmann Institute of Science.

[1] Abbreviations: Az, azurin; ET, electron transfer; HEPES, 4-(2-hydroxyethyl)-1-piperazineethanesulfonic acid; LRET, long-range electron transfer; F114A, Phe114Ala azurin mutant; M121L, Met121Leu azurin mutant; W48L, Trp48Leu azurin mutant; W48M, Trp48Met azurin mutant; wt, wild type.

0006-2960/93/0432-7317$04.00/0

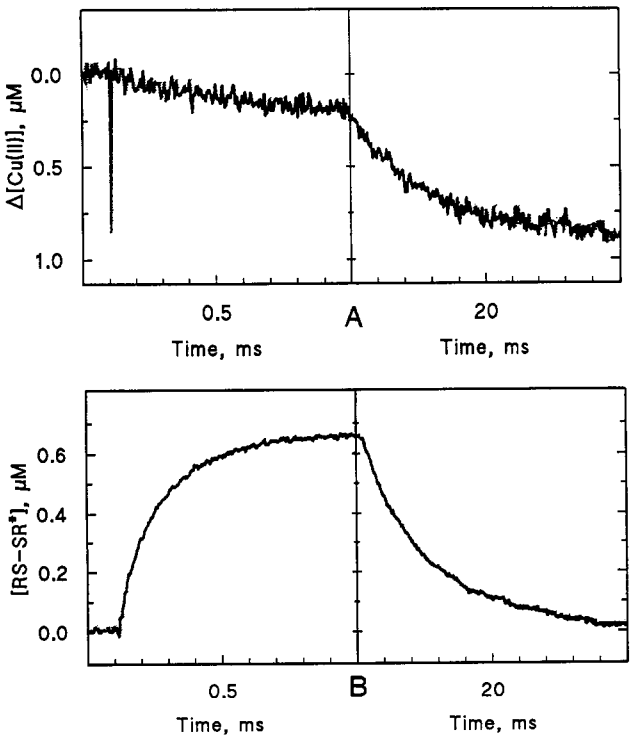

FIGURE 1: Time course of the observed absorbance changes of the mutant W48L following a pulse of accelerated electrons. (A, top) Changes in Cu(II) concentration ($\Delta Cu(II) \equiv [Cu(II)]_0 - [Cu(II)]_t$) monitored at 625 nm ($\epsilon$ = 5.9 mM^{-1} cm^{-1}). (B, bottom) Changes at 410 nm, expressed as $RSSR^-$ concentration (ϵ = 10 mM^{-1} cm^{-1}). Conditions were as follows: temperature, 34.0 °C; pH, 7.0; pulse width, 0.5 (A) and 0.3 μs (B).

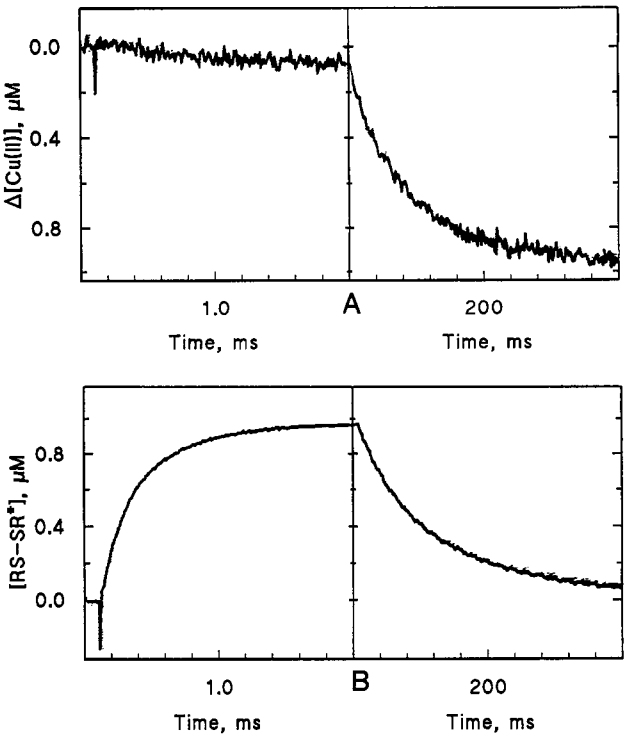

FIGURE 2: Time course of the observed absorbance changes of the mutant W48M following a pulse of accelerated electrons. A (top) and B (bottom) show concentration changes derived from 625- and 410-nm absorbance data, respectively. The data are displayed as in Figure 1. Conditions were as follows: temperature, 4.9 °C; pH, 7.0; pulse width, 0.3 μs.

are analyzed and discussed in terms of the above parameters governing the reaction rates.

MATERIALS AND METHODS

Strains, Plasmids, DNA Techniques, and Protein Production. The *Escherichia coli* strains, DNA constructs, and techniques employed in producing the single-site-mutated azurins have been described (Karlsson et al., 1989b). Similarly, the methods for *E. coli* cultivation and azurin purification have also been reported previously (Pascher et al., 1989). The copper content of the mutants tended to be less than stoichiometric. This was particularly so for the Trp48 mutants, which in some cases contained down to 0.25 Cu per protein molecule. The copper content was determined from the ratio of A_{625}/A_{280}. The extinction coefficient at 625 nm was obtained from the integrated EPR spectra. By analogy to the results obtained for *Ps. aeruginosa* azurin expressed in *E. coli*, zinc ions are bound to the type 1 copper center whenever the latter metal ion is limited (Nar et al., 1992). The high Zn content is thus not the result of a structural peculiarity in the mutated azurins. Since intramolecular ET is not possible in Zn-substituted azurin, no effort was made to separate it from Cu(II) azurin.

Reduction Potentials. The reduction potentials were measured with the optically transparent thin-layer electrolysis (OTTLE) technique to be described in detail elsewhere (Pascher et al., 1993).

Kinetic Measurements. Pulse radiolysis experiments were carried out using the Varian V-7715 linear accelerator of the Hebrew University in Jerusalem. Electrons accelerated to 5 MeV were employed using pulse lengths in the range from 0.1 to 1.5 μs, equivalent to 0.6–10 μM CO_2^- radical ions. All optical measurements were carried out anaerobically under purified argon at a pressure slightly in excess of 1 atm in a 4 × 2 × 1 cm Spectrosil cuvette. Three light passes were applied, which resulted in an overall optical path length of 12.3 cm. A 150-W xenon lamp produced the analyzing light beam, and the appropriate optical filters with cutoffs at 385 or 590 nm were used to avoid photochemistry and light scattering. The data acquisition system consisted of a Tektronix 390A/D transient recorder and a PDP1123 minicomputer. The temperature of the reaction solutions was controlled by a thermostating system and continuously monitored by a thermocouple attached to the cuvette. Practically all reactions were performed under pseudo-first-order conditions, with typically a 10-fold excess of oxidized protein over reductant. Each kinetic run was repeated at least three times.

Aqueous solutions, 0.1 M in sodium formate (pH 4.0), were deaerated and saturated with N_2O in glass syringes. The concentrated protein stock solution was added, and the pH was adjusted to the required value by titration with 0.5 or 0.05 M NaOH. N_2O bubbling was continued for another 5 min, and the solution was then transferred into the pulse radiolysis cell under anaerobic conditions.

Molecular Modeling. Coordinates for wt *Ps. aeruginosa* azurin at 1.9-Å resolution were kindly provided by Dr. H. Nar et al. (1991a) and used as the starting structure for the molecular modeling of the mutant proteins. The general structure of single-residue-mutated azurins has been shown to be close to the structure of the native protein (Nar et al., 1991b), and only changes at the mutated residue and its surroundings, approximately 0.5 nm, were considered in the calculations. Introduction of mutations in the shell around the copper ligands has no gross effect on the overall structure of the metal site (Nar et al., 1991b), and therefore the Cu(II) atom and its ligating atoms were kept fixed.

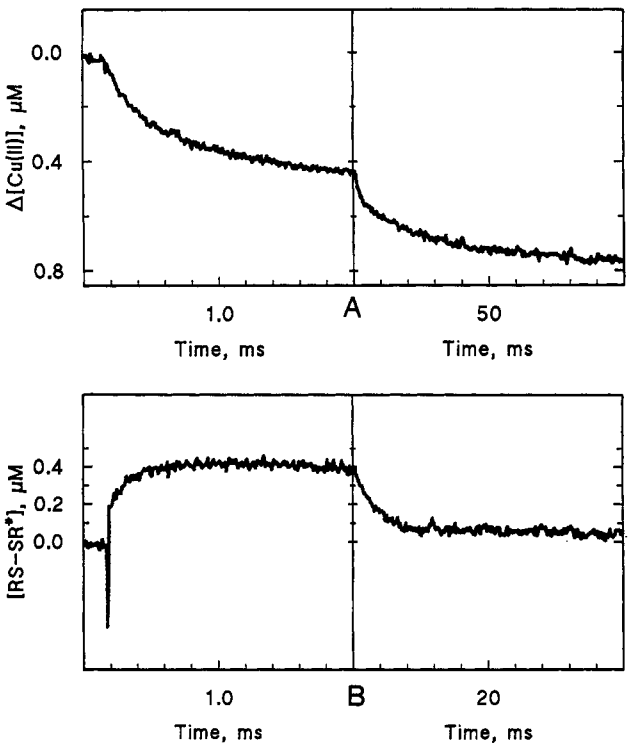

FIGURE 3: Time course of the observed changes of the mutant F114A following a pulse of accelerated electrons. A (top) and B (bottom) show concentration changes derived from 625- and 410-nm absorbance data, respectively. The data are displayed as in Figure 1. Conditions were as follows: temperature, 14.8 (A) and 33.8 °C (B); pH, 7.0; pulse width, 1.0 μs.

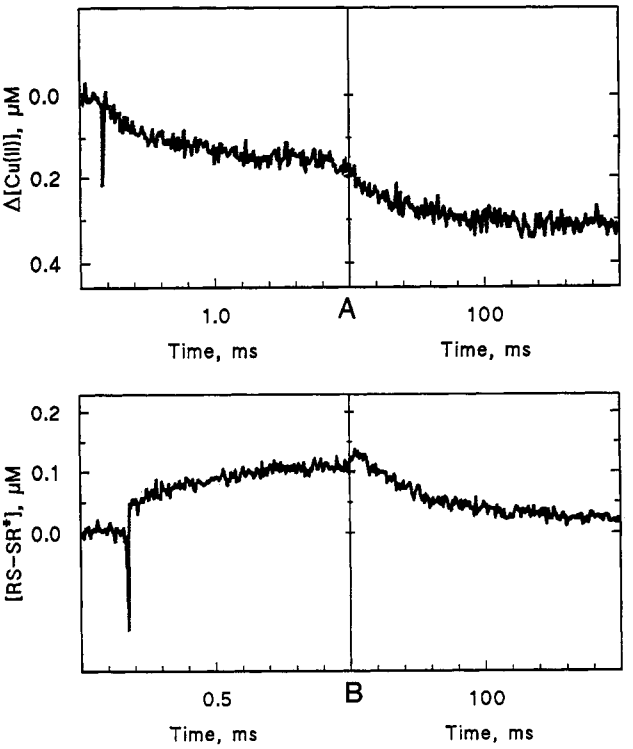

FIGURE 4: Time course of the observed absorbance changes of the mutant M121L following a pulse of accelerated electrons. A (top) and B (bottom) show concentration changes derived from 625- and 410-nm absorbance data, respectively. The data are displayed as in Figure 1. Conditions were as follows: temperature, 14.7 (A) and 7.2 °C (B); pH, 7.0; pulse width, 1.0 (A) and 0.1 μs (B).

The molecular modeling (energy minimization and molecular dynamics) was performed with the programs Discover and InsightII (Biosym Tech., San Diego, CA) applying the consistent valence force field (Dauper-Osguthorpe et al., 1988), excluding cross-term energies and Morse potentials. The steepest-descent and the conjugated-gradients minimization algorithms were used until a maximum derivative of less than 1.2 kJ (mol·nm)$^{-1}$ was achieved. Molecular dynamic calculations were performed in order to overcome local energy minima. The Leapfrog integration algorithm typically was used with 200 iterations at 1000 K and 1.0-fs time steps.

The minimizations were started with all atoms fixed except those in the "new" side chain, after the neighboring side chains were allowed to shift. This procedure was repeated until the interaction energy of all residues (side chain and backbone) and water molecules within 0.5 nm was minimized.

Electron-Transfer Pathways. Electron-transfer pathways were calculated for native and mutated azurins with the program Pathways 2.1 (Beratan et al., 1990, 1991, 1992). The program uses a combination of covalent bonds (C), hydrogen bonds (H), and through-space jumps (S) to link the donor and the acceptor in an LRET process. Each kind of link (C, H, S) is assigned a certain decay parameter, and the overall electron-transfer probability is calculated as the product of decay factors (Beratan et al., 1991).

RESULTS

All reactions were performed in N_2O-saturated aqueous solutions containing 10 mM phosphate and 0.10 M formate, both as sodium salts. Under these conditions, the primary products of water decomposition by the radiation pulse are practically all converted to CO_2^- radicals (Hart & Anbar, 1970). With azurin present in the solution, the CO_2^- radicals were found to react rapidly with two redox-active sites of the protein: the Cu(II) ion and the disulfide bridge. This is shown by the fast absorbance decay observed at 625 nm which is the maximum of the Cu(II) site absorption (Figures 1A–4A, left sides). The rate of this decay was found to depend on both CO_2^- and Az[Cu^{II}] concentration. Hence, this absorption change was assigned to a direct bimolecular reduction of the Cu(II) center by the CO_2^- radicals. On a similar fast time scale, the formation of an absorption band with a maximum at 410 nm was observed (Figures 1B–4B, left sides). This band has been shown to be due to reduction of the disulfide bridge producing an $RSSR^-$ radical ion (Faraggi & Klapper, 1988).

There is a noticeable difference in the behavior of the mutants in this reaction phase: In the two Trp mutants (W48L and W48M), the amplitude of the direct Cu(II) reduction by CO_2^- is rather limited; the yield of $RSSR^-$ is 4 times higher than that of Cu(I) (Figures 1 and 2). This could be an effect of the low copper content of these mutants. For the two other mutants (F114A and M121L), yields of the two fast reduction processes are considerably larger and approximately equal, as shown in Figures 3 and 4.

The transient $RSSR^-$ species decays on a slower time scale (Figures 1B–4B, right sides), and a parallel further decrease in the 625-nm absorption was observed (Figures 1A–4A, right sides) with practically the same rate and amplitude as that of the $RSSR^-$ disappearance. The rate constants for both of these processes are independent of the CO_2^- concentration (in the range 0.6–10 μM) and of the protein concentration (in the range 4–22 μM) of all mutants. We may therefore conclude that an electron is indeed transferred intramolecularly to Cu(II) from $RSSR^-$ in all azurins studied.

In the absence of other intramolecular electron acceptors (i.e., in apo-Az or Az[Cu^I]), the disulfide radical anions dismutate in a bimolecular process with a rate constant at 25

Table I: Reduction Potentials and Rate Constants (k) for the Intramolecular LRET in Wild-Type and Mutated *Ps. aeruginosa* Azurins[a]

azurin	$E^{\circ\prime}$ pH 7, 298 K (mV)	k (s^{-1}) pH 7, 298 K	low pH[c] (temp (K))	high pH[c] (temp (K))
wild type	294	44 ± 7	285 (298)	30 (298)
W48L	323	40 ± 4	100 (286)	15 (286)
W48M	312	33 ± 5	105 (287)	12 (287)
F114A	358	72 ± 14	420 (294)	35 (294)
M121L	412[b]	38 ± 7	410 (294)	20 (294)

[a] Wild-type rate constants are from Farver and Pecht (1989). [b] Measured in HEPES instead of formate. The effect of this substitution has been found to be less than 15 mV for the other mutants. [c] Determined from curve fitting of the rate constants at different pH values extrapolated to low and high pH, respectively.

Table II: Thermodynamic Parameters for the Intramolecular Reduction of Cu(II) by $RSSR^-$

azurin	$-\Delta G^{\circ}$ [a] (kJ mol^{-1})	ΔH^* (kJ mol^{-1})	ΔS^* (J K^{-1} mol^{-1})
wild type	67.9 ± 2.9	47.5 ± 4.0	−56.5 ± 7.0
W48L	70.7 ± 3.1	48.3 ± 0.9	−51.5 ± 5.7
W48M	69.7 ± 3.0	48.4 ± 1.3	−50.9 ± 7.4
F114A	74.1 ● 3.3	52.1 ± 1.3	−36.1 ± 8.2
M121L	79.3 ± 3.5	45.2 ± 1.3	−61.5 ± 7.2

[a] Calculated using a reduction potential for $RSSR/RSSR^-$ of −410 mV (Faraggi & Klapper, 1988). T = 298 K.

°C of 1×10^6 M^{-1} s^{-1} (Farver & Pecht, 1989; O. Farver, & I. Pecht, unpublished results). Similarly, in Az[Zn^{II}], the metal ion has a d^{10} electron configuration and is thus incapable of acting as an electron acceptor under the present conditions. Hence, the bimolecular process is easily discerned from the intramolecular ET.

The rate constants for the intramolecular electron transfer in the different azurin mutants at pH 7.0 and 298 K are summarized in Table I, together with their respective Cu^{II}/Cu^{I} reduction potentials. The temperature dependence of the specific rates of the intramolecular electron-transfer processes is shown in Figure 5, and the calculated activation parameters are summarized in Table II.

Pathway calculations were based on the high-resolution three-dimensional structure of *Ps. aeruginosa* (Nar et al., 1991a) and on the structure calculations of the four mutant azurins. Direct structural studies have demonstrated that mutations outside the copper coordination shell have little effect on the structure of the metal site (Nar et al., 1991b). This observation is supported by optical absorption and EPR studies of a large number of single-site-mutated azurins (Pascher et al., 1993), including the ones studied here. Thus, the EPR spectra are almost identical. For W48L and W48M, $g_{\parallel}$ is shifted from 2.259 in native *Ps. aeruginosa* azurin to 2.253 and 2.261, respectively, while $g_{\perp}$ changes from 2.059 to 2.054 and 2.056, respectively. Further, the characteristic small hyperfine coupling parameter, $A_{\parallel}$, is, within experimental error, the same for all three proteins ($A_{\parallel}$ = 50 G). Also, the position of the maximum of the intense blue band is, within experimental error, the same for these proteins. All of these observations indicate that the copper site in the Trp48 mutants is not significantly modifed relative to the wild-type azurin, in accordance with the above-mentioned observation by Nar et al. (1991b).

The pathway calculations predict very similar electron-transfer rates in the native and all mutated proteins. Two main pathways were found with small variation in the decay factors, ϵ, between the wild-type and the mutated azurins (Table III). One distinct pathway is through the backbone from Cys3 to Asn10 followed by a hydrogen bond from the backbone C=O to the N(3)H of the imidazole copper ligand (His46) (Figure 6). The other pathway goes directly from Cys3 to Thr30 via a hydrogen bond and then from Val31 to Trp48 (or, in the mutants, Met48 and Leu48, respectively) via a through-space jump of about 0.4 nm. Then Val49 is connected to Phe111 by another hydrogen bond, followed by backbone connection to the copper ligand Cys112 (Figure 6).

Table III: Product of the Decay Factors ($\prod \epsilon_f$) for the Two Main Electron-Transfer Pathways from the Disulfide Radical to the Cu(II) in Azurin

azurin	$\prod \epsilon_f \times 10^8$ through backbone[a]	via residue 48[b]
wild type	24.6	2.6
W48L	24.6	4.0
W48M	24.6	3.4
F114A	31.2	3.0
M121L	31.4	2.7

[a] This pathway includes 27 covalent bonds and 1 H-bond. [b] This pathway includes 19 covalent bonds, 2 H-bonds, and 1 through-space van der Waals interaction.

The pH dependence of the LRET rate from $RSSR^-$ to Cu(II) was investigated for all of the azurin mutants over the range 4.8–9.0. The specific rates exhibited identical strong pH dependences with an apparent pK_a of 6.2. At the low and high ends of the examined pH range, the rate constants level off at values given in Table I.

DISCUSSION

The temperature dependence of the intramolecular ET rate constants (Table II and Figure 5) can be analyzed in terms of the Marcus equation for electron exchange between spatially fixed and oriented redox sites (Marcus & Sutin, 1985):

$$\ln \frac{k}{T} = \ln \frac{k_B}{h} + \ln \kappa - \frac{\Delta G^*}{RT} \quad (1)$$

For nonadiabatic processes the electronic transmission coefficient is given by

$$\ln \kappa = -\beta(r - r_0) \quad (2)$$

and the activation free energy is

$$\Delta G^* = \Delta H^* - T\Delta S^* = \frac{\lambda}{4}\left(1 + \frac{\Delta G^{\circ}}{\lambda}\right)^2 \quad (3)$$

Here k_B is the Boltzmann constant, h is Planck's constant, κ is the electronic transmission coefficient, β is the exponential decay factor, and λ is the total reorganization energy.

The slope of the Eyring plots (Figure 5) is $\Delta H^*/R$, and the intercept equals $-[\ln (k_B/h) + \Delta S^*/R]$, where $\Delta S^* = \Delta S^* - R\beta(r - r_0)$. Thus, with β and $(r - r_0)$ known, ΔG^* and λ can be calculated. Earlier data for the wild-type *Ps. aeruginosa* azurin were analyzed according to eqs 1–3, yielding ΔG^* = 4.9 kJ mol^{-1} and λ = 117 kJ mol^{-1} (Farver & Pecht, 1989).

The usefulness of pathway calculations obviously depends on reliable structural data. As noted above (cf. Results), changes in the three-dimensional structure of the single-site-mutated proteins were found to be confined to the mutation site (Nar et al., 1991b; Pascher et al., 1993). On the basis of our pathway calculations, which suggest that the same route is used for LRET from $RSSR^-$ to Cu(II) in all azurins studied so far (Table III and Figure 6), the data collected in this work allow a different analytic approach that yields independent values for both the reorganization energy and the electronic

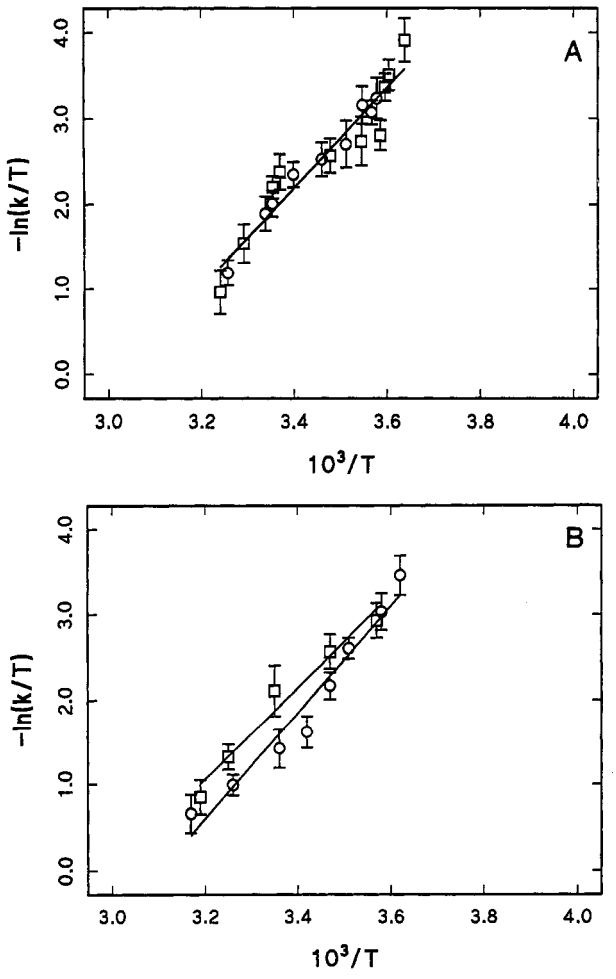

FIGURE 5: Eyring plots of the specific rates of the intramolecular electron transfer from RSSR⁻ to Cu(II): (A, top) W48L (○) and W48M (□); (B, bottom) F114A (○) and M121L (□).

factor. The substitution of Phe with Ala in the F114A mutant is a relatively conservative one, so we may assume that both κ and λ would be the same for the wild-type protein and this mutant. Combining thermodynamic data (Table II) for native *Ps. aeruginosa* and F114A azurins, we calculate $\lambda = 135 \pm 20$ kJ mol^{-1} and $\ln \kappa = -22.5 \pm 0.3$. This is in good agreement with what we calculated earlier for wt azurin (Farver & Pecht, 1989). For the two Trp48 mutants we may also assume that λ is the same for both wt and F114A azurin. We then find that $\ln \kappa$ takes the same value within 0.1 unit, which is certainly within the experimental error. Thus, for all azurins examined here, we may employ the value, $\ln \kappa = -22.5$. With a through-bond distance (including the 0.28-nm H-bond between Asn10 and His46) of 3.7 nm (i.e., $(r-r_0) = 3.4$ nm) this gives $\beta = 6.6$ nm^{-1}, which is in excellent agreement with the experimentally determined decay factor for electron tunneling in ruthenated cytochromes (6.8 nm^{-1}) (Beratan et al., 1990; Onuchic et al., 1992) (cf. Figure 6, insert) and the one calculated for tunneling through a saturated $(CH_2)_n$ chain (6.5 nm^{-1}) (Broo & Larsson, 1990). With this value of $\ln \kappa$, we may finally calculate the reorganization energy in the M121L mutant and find it to be 13 kJ larger than for the other mutants. In this mutant, the copper-ligating Met121 is substituted with a nonligating leucine residue which may alter the reorganization energy, counteracting the increase in rate expected on the basis of the larger driving force (cf. Table II).

The nature of biological LRET in proteins is still a matter of discussion. While there is substantial evidence for through-bond ET (Beratan et al., 1990, 1991, 1992; Farver & Pecht, 1992; Farver et al., 1992; Onuchic et al., 1992), Moser et al. (1992) recently analyzed data obtained from a large variety of intramolecular electron-transfer reactions and found that the free energy optimized rate constants for many "biological" ET processes correlate well with the edge-to-edge distance between donor and acceptor, with a decay factor $\beta = 14$ nm^{-1}. From the refined *Ps. aeruginosa* azurin structure (Nar et al., 1991a), the distance $(r-r_0)$ between S_γ of Cys26 and S_γ of Cys112, which represents the shortest edge-to-edge distance between electron donor and acceptor, is 2.46 nm. This gives $\beta = 9$ nm^{-1}. The difference in the above β-values is too large to be accounted for in terms of experimental error. Further, the calculated maximum LRET rate constant for azurin (i.e., for $\lambda = -\Delta G°$) is 10^3 s^{-1}, but using the correlation line of Moser et al. (1992) the rate constant should be 2 orders of magnitude smaller. We may therefore conclude that our data do not fit an exponential decay correlation with direct through-space distance. Instead, $k_{MAX} = 10^3$ s^{-1} fits perfectly on a linear plot of log k_{MAX} vs the through-bond distance for Ru-substituted cytochrome *c* drawn with a slope of 6.7 nm^{-1} (Figure 6, insert).

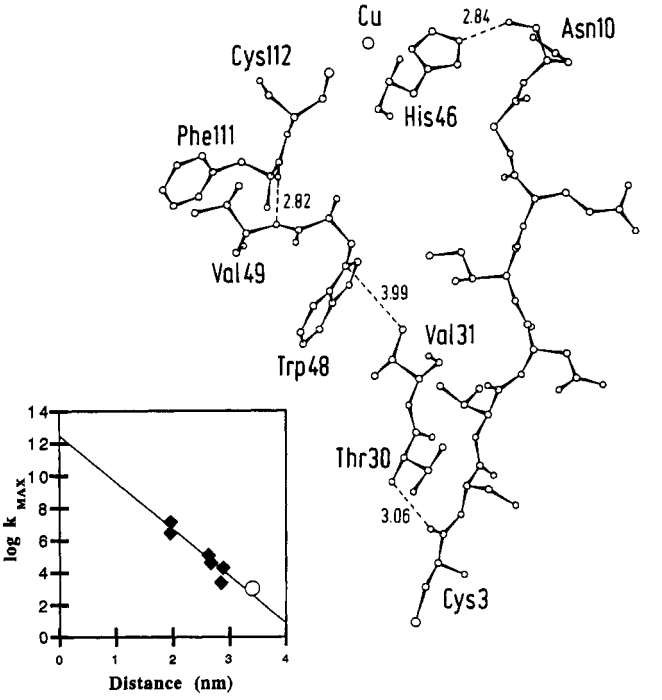

FIGURE 6: Hypothetical pathways for electron transfer from the sulfur of Cys3 to the copper ligands Cys112 and His46. Some interconnecting distances (in angstroms) are shown (see text). In the mutants, Trp48 is replaced by Met or Leu, and the distances from Val131C_γ to Met48C_γ and Leu48C_γ are then 3.81 and 3.72 Å, respectively. Insert: Plot of log k_{MAX} vs the through-bond distance. The solid points (■) represent Ru-modified cytochromes (Onuchic et al., 1992), and the open circle is the k_{MAX} for wt azurin. The line is the theoretical one with $\beta = 6.6$ nm^{-1}.

Recent studies of wild-type azurins isolated from different bacteria suggested that Trp48 may be involved in LRET (Farver & Pecht, 1992). Therefore, the effect on the LRET rate of substituting the indole ring by a nonaromatic side chain, resolved in the present studies, is unexpectedly small. However, the pathway calculations (Table III) are consistent with this residue not being involved, as the route including Trp48 has a decay factor about 10 times smaller than that of the longer route via the backbone. This suggests that the pathway involving residue 48 only plays a minor role for LRET in the azurins studied here.

It should also be kept in mind that the above calculation does not resolve between pathways involving π- and σ-orbital systems. In an earlier theoretical analysis, Broo and Larsson (1991) applied an extended Hückel method to the same LRET reaction and the same pathways. In contrast to the present results, they found that the route involving Trp48 is 10 times more efficient than the route through the backbone. However, their conclusions were somewhat indecisive in that removal of the Trp48 indole ring reduced the rate 5-fold, but removal of two additional aromatic rings (Phe15 and Phe29) restored the rate to that of wild-type protein. In addition, only unrefined coordinates were available for this calculation, and the removal of the aromatic residues was made with no readjustment of the structure. Hence, further calculations are required before a better comparison between the two computational procedures can be made. Also, a crystal structure determination of the W48M mutant is under way (L. Sjölin, to be published). This would provide an independent examination of the validity of the present molecular modeling.

In discussing the examined LRET between $RSSR^-$ and Cu(II) in azurin, one should also keep in mind that this process is most likely a nonphysiological one, and its pathway is not a product of evolutionary optimization. In fact, the disulfide is situated in a "cold" spot on the azurin molecule, as nicely illustrated by Beratan et al. (1991, 1992). In systems that were selected for efficient electron transfer, aromatic residues may be positioned so as to considerably increase the electronic coupling. Examples of this are the tryptophan-mediated reduction of quinone in the photosynthetic reaction center (Plato et al., 1989) and Tyr83 in plastocyanin (He et al., 1991).

In all four azurin mutants studied, we observed a decline in the rate of the intramolecular LRET with increasing pH (Table I), with a pK_a value of 6.2. Practically the same pH dependence of the intramolecular electron-transfer rate has been observed for all other azurins studied so far (Farver & Pecht, 1989, 1992). The reduction potential of Cu^{II}/Cu^{I} in the wild-type and mutant azurins studied here also decreases at higher pH by about 50 mV and with a similar apparent pK_a (Pascher et al., 1993), which would make the driving force smaller and the rate lower. However, with the values for the reorganization energy obtained above, the change in potential could be the cause for only a fraction of the observed change in the rates. Indirect structural changes induced by variations in pH, such as those described by Nar et al. (1991a), could be more important in that they might affect both λ and the electronic transmission coefficient, κ.

Perhaps a more likely origin of the pH dependence of the rates is the protonation state of Asp23. This residue is conserved in all azurins where this pH dependence was observed, but is absent in *Alcaligenes sp.* azurin which lacks this large pH dependence (O. Farver, & I. Pecht, unpublished observations). There are no other sequence differences in this region besides at position 23 which could account for this effect. The protonation state of the Asp23 carboxylate, which is in close proximity to the disulfide bridge, could markedly affect the driving force of the reaction. Further studies on azurin mutants may resolve the cause for this marked pH dependence of the LRET.

ACKNOWLEDGMENT

Thanks are due to Professor R. Huber and Dr. H. Nar for providing us with the azurin coordinates. The authors thank Dr. D. N. Beratan for help with the pathway calculations and Professors H. B. Gray and S. Wherland for their interest in this work and many helpful discussions.

REFERENCES

Adman, E. T. (1985) in *Topics in molecular and structural biology: Metalloproteins* (Harrison, P. M., Ed.) pp 1–42, Chemie Verlag, Weinheim, Germany.

Baker, E. N. (1988) *J. Mol. Biol. 203*, 1071–1095.

Beratan, D. N., Onuchic, J. N., Betts, J. N., Bowler, B. E., & Gray, H. B. (1990) *J. Am. Chem. Soc. 112*, 7915–7921.

Beratan, D. N., Betts, J. N., & Onuchic, J. N. (1991) *Science 252*, 1285–1288.

Beratan, D. N., Betts, J. N., & Onuchic, J. N. (1992) *J. Phys. Chem. 96*, 2852–2855.

Broo, A., & Larsson, S. (1990) *Chem. Phys. 148*, 103–115.

Broo, A., & Larsson, S. (1991) *J. Phys. Chem. 95*, 4925–4928.

Clarke, M. J., Goodenough, J. B., Ibers, J. A., Jørgensen, C. K., Mingos, D. M. P., Neilands, J. B., Palmer, G. A., Reinen, D., Sadler, P. J., Weiss, R., & Williams, R. J. P. (Eds.) (1991) *Long-Range Electron Transfer in Biology; Struct. Bonding 75*, 1–225.

Dauper-Osguthorpe, P., Roberts, V. A., Osguthorpe, D. J., Wollf, J., Genest, M., & Hagler, A. T. (1988) *Proteins: Struct. Funct. Genet. 4*, 31–47.

Faraggi, M., & Klapper, M. H. (1988) *J. Am. Chem. Soc. 110*, 5753–5756.

Farver, O., & Pecht, I. (1984) in *Copper proteins and copper enzymes* (Lontie, R., Ed.) Vol. 1, pp 183–214, CRC, Boca Raton, FL.

Farver, O., & Pecht, I. (1989) *Proc. Natl. Acad. Sci. U.S.A. 86*, 6968–6972.

Farver, O., & Pecht, I. (1992) *J. Am. Chem. Soc. 114*, 5764–5767.

Farver, O., Skov, L. K., van de Kamp, M., Canters, G. W., & Pecht, I. (1992) *Eur. J. Biochem. 210*, 399–403.

Hart, E. J., & Anbar, M. (1970) *The hydrated electron*, Wiley, New York.

He, S., Modi, S., Bendall, D. S., & Gray, J. C. (1991) *EMBO J. 10*, 4011–4016.

Karlsson, B. G., Aasa, R., Malmström, B. G., & Lundberg, L. G. (1989a) *FEBS Lett. 253*, 99–102.

Karlsson, B. G., Pascher, T., Nordling, M., Arvidsson, R. H. A., & Lundberg, L. G. (1989b) *FEBS Lett. 246*, 211–217.

Karlsson, B. G., Nordling, M., Pascher, T., Tsai, L.-C., Sjölin, L., & Lundberg, L. G. (1991) *Protein Eng. 4*, 343–349.

Marcus, R. A., Sutin, N. (1985) *Biochim. Biophys. Acta 811*, 265–322.

Moser, C. C., Keske, J. M., Warncke, K., Farid, R. S., & Dutton, P. L. (1992) *Nature 355*, 796–802.

Nar, H., Messerschmidt, A., Huber, R., van de Kamp, M., & Canters, G. W. (1991a) *J. Mol. Biol. 221*, 765–772.

Nar, H., Messerschmidt, A., Huber, R., van de Kamp, M., & Canters, G. W. (1991b) *J. Mol. Biol. 218*, 427–447.

Nar, H., Huber, R., Messerschmidt, A., Filippou, A. C., Barth, M., Jacquinod, M., van de Kamp, M., & Canters, G. W. (1992) *Eur. J. Biochem. 205*, 1123–1129.

Onuchic, J. N., Beratan, D. N., Winkler, J. R., & Gray, H. B. (1992) *Annu. Rev. Biophys. Biomol. Struct. 21*, 349–377.

Pascher, T., Bergström, J., Malmström, B. G., Vänngård, T., & Lundberg, L. G. (1989) *FEBS Lett. 258*, 266–268.

Pascher, T., Karlsson, B. G., Nordling, M., Malmström, B. G., & Vänngård, T. (1993) *Eur. J. Biochem. 212*, 289–296.

Plato, M., Michel-Beyerle, M. E., Bixon, M., & Jortner, J. (1989) *FEBS Lett. 249*, 70–74.